An Isogenic Blood-Brain Barrier Model Comprising Brain Endothelial Cells, Astrocytes and Neurons Derived from Human Induced Pluripotent Stem Cells

Scott G. Canfield[1], **Matthew J. Stebbins**[1], **Bethsymarie Soto Morales**[1], **Shusaku W. Asai**[1], **Gad D. Vatine**[2], **Clive N. Svendsen**[2], **Sean P. Palecek**[1,*], and **Eric V. Shusta**[1,*]

[1]Department of Chemical and Biological Engineering, University of Wisconsin Madison, Madison, WI 53706

[2]Cedars-Sinai Medical Center, Board of Governors Regenerative Medicine Institute, Los Angeles, CA 90048
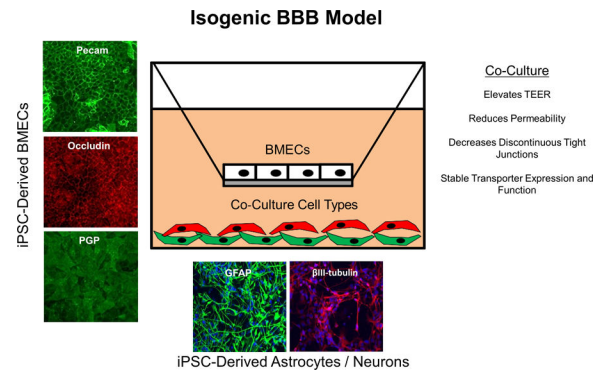
Abstract

The blood-brain barrier (BBB) is critical in maintaining a physical and metabolic barrier between the blood and the brain. The BBB consists of brain microvascular endothelial cells (BMECs) that line the brain vasculature and combine with astrocytes, neurons and pericytes to form the neurovascular unit (NVU). We hypothesized that astrocytes and neurons generated from human induced pluripotent stem cells (iPSCs) could induce BBB phenotypes in iPSC-derived BMECs, creating a robust multicellular human BBB model. To this end, iPSCs were used to form neural progenitor-like EZ-spheres, which were in turn differentiated to neurons and astrocytes, enabling facile neural cell generation. The iPSC-derived astrocytes and neurons induced barrier tightening in primary rat BMECs indicating their BBB inductive capacity. When co-cultured with human iPSC-derived BMECs, the iPSC-derived neurons and astrocytes significantly elevated trans-endothelial electrical resistance (TEER), reduced passive permeability, and improved tight junction continuity in the BMEC cell population, while p-glycoprotein (PGP) efflux transporter activity was unchanged. A physiologically relevant neural cell mixture of 1 neuron: 3 astrocytes yielded optimal BMEC induction properties. Finally, an isogenic multicellular BBB model was successfully demonstrated employing BMECs, astrocytes, and neurons from the same donor iPSC source. It is anticipated that such an isogenic facsimile of the human BBB could have applications in furthering understanding the cellular interplay of the NVU in both healthy and diseased humans.

Graphical Abstract

---

[*]Corresponding authors: Eric V. Shusta, Department of Chemical and Biological Engineering, University of Wisconsin-Madison, 1415 Engineering Drive, Madison, WI 53706, shusta@engr.wisc.edu, Ph: (608) 262-1092, Fax: (608) 262-5434, Sean P. Palecek, Department of Chemical and Biological Engineering, University of Wisconsin-Madison, 1415 Engineering Drive, Madison, WI 53706, palecek@engr.wisc.edu, Ph: (608) 262-8931, Fax: (608) 262-5434.

Isogenic BBB Model

iPSC-Derived BMECs

Pecam

Occludin

PGP

BMECs

Co-Culture Cell Types

Co-Culture

Elevates TEER

Reduces Permeability

Decreases Discontinuous Tight Junctions

Stable Transporter Expression and Function

GFAP

βIII-tubulin

iPSC-Derived Astrocytes / Neurons

We developed an isogenic human blood-brain barrier (BBB) model comprising induced pluripotent stem cell (iPSC) derived brain endothelial cells (BMECs), astrocytes and neurons. We have demonstrated that iPSC-derived neurons and astrocytes can improve the tight junctions and induce barrier tightening in iPSC-derived BMECs. An isogenic BBB model where each cell type is derived from the same patient iPSC source would enable new approaches in brain disease modeling and drug development.

Keywords

blood-brain barrier model; neurovascular unit; astrocytes; neurons; stem cells

Introduction

The blood brain barrier (BBB) is key for healthy brain activity and is formed by specialized endothelial cells that line the cerebral vasculature. These brain microvascular endothelial cells (BMECs) form a barrier that regulates the transport of nutrients, metabolites and cells between the blood and brain while also helping to protect the central nervous system from toxic and pathogenic insults. The barrier phenotype is elicited through the expression of a specialized cohort of tight junction proteins, efflux transporters, and nutrient transporters (Zhao *et al.* 2015). In healthy conditions, the BBB is effective in maintaining the delicate homeostasis between the blood and brain; however in a number of diseases, such as stroke, Alzheimer's, and ALS, BBB dysfunction can play a significant role in disease progression (Zlokovic 2008).

A number of *in vitro* BBB models have been developed to help elucidate the role of the BBB in brain development, function, and disease, and to develop potential therapeutic approaches. Freshly isolated BMECs from various animal sources have been successfully employed, although species variations must be considered when interpreting these results and comparing them to the human condition (Deli *et al.* 2005, Warren *et al.* 2009, Syvänen *et al.* 2009). Additionally, freshly isolated human BMECs and immortalized BMECs have been used to model the BBB (Cecchelli *et al.* 2007, Weksler *et al.* 2005). However, primary and transformed BMECs tend to de-differentiate and have decreased barrier properties once they are removed from the brain microenvironment (Weksler et al. 2005, Förster *et al.* 2008, Man *et al.* 2008, Calabria & Shusta 2008).

Some of the limitations of BBB models can be mitigated by including other cells of the neurovascular unit (NVU) such as astrocytes, neurons or pericytes to help provide cues that are critical in the development, maintenance, and regulation of unique BBB properties. By creating such multicellular *in vitro* BBB models that better approximate the more complex NVU, study of BBB function in healthy and diseased states can become more representative of *in vivo* BBB physiology. A main focus of developing multicellular BBB models has been investigating the interplay between astrocytes and BMECs (Janzer & Raff 1987). Primary astrocytes in co-culture enhance BBB properties, including increased TEER and reduced paracellular permeability (Deli et al. 2005). More recently, pericytes in co-culture have been shown to have similar BBB enhancing effects to astrocytes (Nakagawa *et al.* 2007, Lippmann *et al.* 2014). Neurons have also been shown to stimulate continuous tight junction formation in BMECs following co-culture (Savettieri *et al.* 2000, Schiera *et al.* 2003, Brown *et al.* 2015). Moreover, the multicellular combination of pericytes, astrocytes, and neurons has been found to induce BMEC phenotypes more significantly than any single co-cultured cell type (Nakagawa *et al.* 2009, Lippmann *et al.* 2011, Lippmann *et al.* 2012, Brown et al. 2015).

To address properties such as scale, human sourcing, and human disease modeling as they relate to *in vitro* BBB models, our group recently developed an approach to differentiate human iPSCs to BMEC-like cells (Lippmann et al. 2012, Wilson *et al.* 2015). These iPSC-derived endothelial cells exhibit a number of important BBB characteristics including elevated trans-endothelial electrical resistance (TEER), reduced fluorescein permeability, active efflux transporters, and the expression of nutrient transporters and tight junction proteins (Wilson et al. 2015, Lippmann et al. 2012, Lippmann et al. 2014, Lippmann *et al.* 2013). Since other peripheral endothelia can also express some of the markers and phenotypes characteristic of BMECs, we refer to these iPSC-derived cells as being BMEC-like (abbreviated as iPSC-derived BMECs) (Lippmann et al. 2012, Wilson *et al.* 2015). In addition, we demonstrated that co-culture with NVU cells including primary human brain pericytes, astrocytes, and neurons in various combinations induced BBB properties such as barrier tightening in iPSC-derived BMECs (Lippmann et al. 2014, Lippmann et al. 2012). However, the co-cultured NVU cells were of primary origin, and hence limited in scale and accessibility.

Here, we hypothesized that it would be possible to differentiate iPSCs to astrocytes and neurons that are capable of inducing BBB phenotypes in isogenic iPSC-derived BMECs. Such an isogenic human NVU model derived from the same human donor could provide substantial benefits in the study of BBB structure and function in healthy and diseased patients. To this end, we employed EZ spheres, a stable and expandable pluripotent stem cell-derived neural stem cell-like aggregate system (Ebert *et al.* 2013, Sareen *et al.* 2014). iPSC-derived EZ spheres retain their potential to form neural rosettes following prolonged cultures and can be differentiated into various neural and glial lineages (Ebert et al. 2013). We demonstrate that primary or iPSC-derived BMECs in co-culture with EZ sphere-derived astrocytes and/or neurons exhibit reduced permeability and improved tight junction localization compared to BMECs in monoculture. Furthermore, iPSC-derived astrocytes and neurons increased BMEC TEER to greater levels than co-culture with primary human NPC-derived astrocytes and neurons, or rat astrocytes. Finally, we demonstrate the capability for

isogenic NVU modeling by employing BMECs, astrocytes and neurons differentiated from the same patient-derived iPSC line.

Materials and Methods

iPSC differentiation to BMECs

IMR90-4 (WiCell) and CS03iCTRn2 (Cedars Sinai iPSC-Core) iPSCs were cultured between passages 32–56 on Matrigel (BD Biosciences) and supplemented daily with mTESR1 medium (WiCell) as previously described (Stebbins *et al.* 2015, Yu *et al.* 2007). iPSC line, CS03iCTRn2 was generated at Cedars Sinai iPSC-Core and was verified for pluripotency markers, array based Pluri-Test, and G-band karyotype analysis. iPSCs were passaged every 3–4 days with Versene (Life Technologies) at a typical ratio of 1:12. BMECs were differentiated following seeding of iPSCs singularized with Accutase (Life Technologies) at a seeding density of 10,000 cells/cm^2 and expanded to 30,000 cells/cm^2 (2–3 days)(Wilson et al. 2015). Once the optimal density (30,000 cells/cm^2) was reached, medium was replaced with unconditioned medium (UM: 100 mL Knock-out serum replacement (Life Technologies), 5 mL non-essential amino acids (Life Technologies), 2.5 mL of gluta-max (Life Technologies), 3.5 uL of β-mercapto-ethanol (Sigma), and 392.5 mL of DMEM/F12 (1:1) daily for six days. UM was then replaced with EC medium containing 200 mL hESFM (Life Technologies) supplemented with 20 ng/mL basic fibroblast growth factor (bFGF; WiCell) and 1% platelet-derived bovine serum (Biomedical Technologies, Inc.) for two days. Cells were then dissociated into single cells with Accutase and plated onto collagen IV (400 ug/mL; Sigma) and fibronectin (100 ug/mL; Sigma) in sterile water at a density of 1×10^6 cells/cm^2 on 1.12 cm^2 Transwell-Clear permeable inserts (0.4 μm pore size; Corning) or at a density of 250,000 cells/cm^2 on 12-/24-/96-well tissue culture polystyrene plates (Corning). The first 24 h following the subculture of the BMECs, the cells were cultured in EC medium and then switched to EC medium lacking bFGF for the duration of the experiments.

iPSC differentiation to EZ-sphere derived neurons and astrocytes

4.2 (GMOO3814 Coriell Institute) and CS03iCTRn2 iPSCs were differentiated into EZ spheres by lifting intact iPSC colonies with collagenase (1 mg/mL, Gibco) in an ultra-low attachment flask (Yu et al. 2007). EZ spheres were fed every other day with an EZ-sphere medium consisting of DMEM/F12 supplemented with 100 ng/mL bFGF, 100 ng/mL epidermal growth factor (EGF, Pepro-tech), and 5 ug/mL heparin (Sigma) and passaged weekly using a mechanical dissociation technique. *EZ-sphere differentiation to neurons*: EZ spheres were singularized with Accutase and seeded at 25,000 cells/cm^2 onto Matrigel coated plates. Cells were cultured in neuron medium consisting of DMEM/F12 (70:30;Life Technologies) supplemented with 1% penicillin-streptomycin, 2% B27 minus vitamin A (Life Technologies) and 2 ug/mL heparin for two weeks with media changes every other day (Ebert et al. 2013). *EZ-sphere differentiation to astrocytes:* EZ spheres were treated with a astrocyte induction medium consisting of DMEM/F12 supplemented with 1% NEAA, 1% N2 (neural supplement), heparin (2ug/mL) and all-trans retinoic acid (RA, 0.5 uM) for 11 days with daily media changes and were renamed astrospheres, due to their propensity to differentiate into astrocytes. The astrospheres could then be transferred back to EZ-sphere

medium and passaged weekly with mechanical dissociation. Astrospheres could be singularized with Accutase and plated onto Matrigel-coated plates at a density of 25,000 cells/cm^2 and cultured in astrocyte medium consisting of DMEM/F12 (1:1, Life Technologies) with 1% NEAA, 1% N2, and 2 ug/mL heparin for two weeks with media changes every other day (Sareen et al. 2014).

Isolation of Rat BMECs

All animal work was performed using protocols approved by the University of Wisconsin-Madison Animal Care and Use Committees and following NIH guidelines for care and use of laboratory animals. Rat brain capillaries were isolated from adult male Sprague Dawley rats (Harlan). The brain tissue was minced and digested in collagenase type-2 (0.7 mg/mL) and DNAse I (39 U/mL). Following centrifugation in 20% bovine serum albumin, the purified microvessel pellet was digested further in 1 mg/mL collagenase/dispase and DNAse I. To obtain a pure capillary population, we utilized a 33% Percoll gradient and plated the cells onto collagen IV/fibronectin-coated Transwells. Capillaries were cultured in DMEM supplemented with 20% PDS, 1 ng/mL bFGF, 1 ug/mL heparin, 2 mM L-glutamine, and 1% antibiotic-antimycotic solution. Pure BMEC monolayers were obtained by treating the cells with puromyocin (4 ug/mL) for two days following seeding. Co-culture experiments began ~ 4 days following isolation at which point the BMECs had reached confluence (Calabria *et al.* 2006).

Isolation of Rat Astrocytes

Astrocytes were harvested as previously described (Weidenfeller *et al.* 2007). P6 neonatal rat's cortices were collected and minced in HBSS media. Trypsin (5 mg/mL) was utilized to digest the cortices for 25 min at 37°C, followed by 5 minutes of DNAse I (114 U/mL). The digested tissue was filtered through a 70 um mesh strainer and seeded at a density of 2.5×10^4 cells/cm^2 in collagen I (50 ug/mL) coated flasks. Astrocytes were cultured in DMEM supplemented with 10% fetal bovine serum, 10% horse serum, L-glutamine (2 mmol/L) and 1% antibiotic-antimycotic.

Culture of 3T3 Fibroblasts and NPCs

3T3 mouse fibroblast cells (ATCC) were cultured in DMEM supplemented with 10% FBS with daily media changes. Mouse 3T3 cells were utilized as a non-neural cell control in the co-culture experiments. Human NPCs (a kind gift of Dr. Guido Nikkhah) were maintained in medium consisting of DMEM/F12 (70:30, Life Technologies) supplemented with 2% B27, 1% antibiotic-antimycotic, 20 ng/mL bFGF, 20 ng/mL EGF, 10 ng/mL leukemia inhibitor factor (LIF; Millipore) and 5 ug/mL heparin (Lippmann et al. 2011). NPCs were passaged every week via mechanical dissociation. NPCs were differentiated to approximately 1:3 neurons: astrocytes by seeding Accutase-singularized cells onto poly-L-lysine (Sigma) coated flasks and culturing in NPC maintenance medium lacking the growth factors and supplemented with 1% FBS for 12 days (Lippmann et al. 2011).

Initiation of Co-Culture experiments

Co-cultures were executed in a similar fashion in all experiments unless otherwise stated. Immediately following the sub-culture stage of the iPSC-BMECs, BMECs were maintained as either a monoculture or co-culture with human stem cell-derived astrocytes, neurons, or varying combinations, 3T3 fibroblasts, primary human NPC-derived astrocytes and neurons, or rat astrocytes. All experimental co-culture groups were seeded at 25,000 cells/cm^2 prior to the initiation of co-culture. BMECs were seeded onto Transwells and all co-culture subtypes were seeded below the Transwells onto the plate surface. For 24 h following the subculture of iPSC-BMECs onto Transwells, all cells were cultured in EC medium (+PDS/ +bFGF) and then transitioned to EC medium (+PDS/−bFGF) for the remainder of all experiments. Additional co-culture media were tested : DMEM/F12 medium (+10% FBS), EC medium (+ 10% FBS), EC medium (+1% FBS), EC medium/DMEM/F12 medium (+10% FBS) 50:50 mix; all experimental media conditions resulted in viable cells, however the greatest barrier tightening was observed when EC medium (+PDS/ +bFGF) was utilized for the first 24 h of co-culture, and then transitioned to EC medium (+PDS/−bFGF). The initiation of co-culture of rat BMECs with human iPSC-derived astrocytes and neurons occurred four days following rat BMEC isolation. Co-culture experiments employing rat BMECs conducted in the rat BMEC medium previously described.

Resistance measurements

Trans-endothelial electrical resistance (TEER) was measured every 24 h following the sub-culture of BMECs. Resistance was recorded using an EVOM ohmmeter with STX2 electrodes (World Precision Instruments). TEER values were presented as Ωxcm^2 following the subtraction of an un-seeded Transwell and multiplication by 1.12 cm^2 to account for the surface area. TEER measurements were measured three independent times on each sample and at least from three triplicate filters for each experimental condition.

Immunocytochemistry and analysis of tight junctions

Immunocytochemistry was conducted on iPSC-BMECs following mono/co-culture conditions and on all experimental groups utilized in co-culture experiments as previously described (Stebbins et al. 2015). Primary antibody sources and dilutions are provided in Supplementary Table 1. Cells were fixed in cold methanol (100%, Sigma) for 15 min. Cells were blocked in 10% goat serum (Sigma) for 30 min at room temperature. Images were taken on Olympus epifluorescence microscope. Primary antibodies, dilution ratios, fixation and blocking agents were previously described (Stebbins et al. 2015). Discontinuous tight junctions were quantified in occludin and claudin-5 immuno-labeled BMECs following monoculture or co-culture with iPSC-derived neurons and astrocytes (1:3 ratio). Following immunostaining with occludin or claudin-5, cells that lacked at least one continuous junction were classified as discontinuous. Images were processed in Image J with a minimum of ten fields with approximately 30 cells/field from three separate differentiations were quantified and all experimental groups remained blinded until completion of the study. Using the same images, the area of each image that exhibited occludin or claudin-5 immunoreactivity was measured to determine the area fraction index.

Western Blot

BMECs were rinsed 1× with PBS and lysed using ice-cold RIPA buffer with protease inhibitor cocktail (Pierce). Lysates were quantified for protein concentration using a BCA assay (Pierce) and loaded into 4–12% Tris-Gyline SDS-page gels (Invitrogen). After transferring samples onto nitrocellulose membranes, the membranes were washed one time with Tris-buffered saline with 0.1% Tween 20 (TBST) and blocked for 1 h in blocking buffer (5% non-fat dry milk dissolved in TBST). Membranes were then probed overnight at 4°C with primary antibodies (Table S1) in blocking buffer. Membranes were washed 3× with 5 mL of TBST, then incubated 10 min with 10 mL of TBST, followed by aspiration of the TBST and incubation of blots again with 10 mL of TBST for 5 min (wash step). Membranes were probed with secondary antibodies diluted in blocking buffer for 1 h at room temperature in the dark (1:5000 donkey anti-mouse IRDye 800CW, LICOR; 1:5000 donkey anti-rabbit 680RD, LICOR). Membranes were subjected to a second wash and were subsequently imaged using a LICOR Odyssey Imager and quantified using the LI-COR Image Studio v2.0.

Flow Cytometry

BMECs or day 14 EZ-sphere derived astrocytes and neurons were incubated with Accutase for 7 min. Cells were gently pipetted from the plate surface and were resuspended in their respective media and counted on a hemocytometer. Cells were centrifuged for 5 min at 1000 g and fixed in 2% paraformaldehyde for 20 min at room temperature. Cells were then incubated in PBS supplemented with 40% goat serum and 0.1% Triton X-100 for 20 min at room temperature. Primary antibodies (Table S1) and control mouse or rabbit IgG at matching concentration were diluted in PBS supplemented with 40% goat serum for 30 min. Following primary antibody incubation, cells were washed three times in PBS containing 1% FBS. Alexa-488 goat anti-rabbit or anti-mouse IgG was added to the cells at a dilution of 1:200 in PBS containing 40% goat serum and incubated for 30 min. Cells were washed three times in PBS supplemented with 0.1% BSA and analyzed using a FACScaliber (BD).

P-glycoprotein efflux transporter activity

For transporter assays, iPSC-BMECs were sub-cultured onto Transwells at a density of 1 million cells/cm^2 and were maintained in monoculture or co-culture for 48 h in EC medium. Rhodamine 1,2,3 (10 uM, Sigma) was utilized as a PGP substrate and cyclosporine A (10 uM, CsA; Sigma) served as a PGP inhibitor. iPSC-BMECs were removed from co-culture conditions for 1 h to conduct Rhodamine 1,2,3 transport studies; no change in TEER was observed. BMECs were pre-incubated with CsA for 1 h at 37°C on a rotating platform. The upper chamber received rhodamine 1,2,3 with or without CsA for 1 h at 37°C on the rotating platform. Following incubation, aliquots were taken from the bottom chamber and fluorescence was quantified on a fluorescent plate reader and normalized to protein content quantified by BCA assay.

Permeability measurements

Sodium fluorescein (10 uM, 376 Daltons; Sigma) was utilized to determine the permeability of the iPSC-BMEC barrier. Following 48 h of monoculture or co-culture, fresh EC medium

was added to the Transwell system, with EC medium containing sodium fluorescein added to the top chamber and EC medium lacking sodium fluorescein added to the bottom chamber. 150 uL aliquots were taken from the bottom chamber at 0, 15, 30, 45, and 60 min, and immediately replaced with pre-warmed EC medium. Permeability coefficients were calculated based on the cleared volume of fluorescein from the top chamber to the bottom chamber.

Statistical Analysis

Data throughout the manuscript are presented as mean ± SD. SigmaStat 3.0 software (Systat Software) was used for statistical analyses. Statistical comparisons were performed using one-way analysis of variance (ANOVA) with Holm-Sidak correction for multiple testing over all comparisons or unpaired Students t-test as appropriate. Figure legends describe the statistical tests used for each particular data set.

Results

Derivation of EZ-sphere derived astrocytes and neurons

Established protocols were used to differentiate astrocytes and neurons from EZ-spheres in a timely and efficient manner (Ebert et al. 2013, Sareen et al. 2014) (Figure 1A.). EZ-spheres were maintained in DMEM F/12 supplemented with bFGF and EGF (EZ Sphere Medium) and were mechanically dissociated weekly. EZ spheres were selectively differentiated toward a neuronal population by culture in DMEM/F12 supplemented with B27 (w/o vitamin A) (Neuron Induction Medium) (Figure 1A). EZ-sphere-derived neurons expressed βIII tubulin, a neuron-specific marker, while astrocyte markers, GFAP, an intermediate filament protein expressed by astrocytes, and S100 calcium binding protein (S100B), a mature glial-specific marker, were completely absent in this population. EZ-sphere-derived neurons were also negative for paired box protein 6 (PAX-6), an early ectoderm marker. EZ-spheres were also differentiated to astrospheres, a neural progenitor population, by Astrocyte Induction Medium supplemented with retinoic acid. Astrospheres were then further differentiated to astrocytes in DMEM/F12 supplemented with N2 (Astrocyte Induction Medium), leading to cell populations exhibiting glial morphology and expressing GFAP and S100B. Further confirming the selective differentiation to the astrocyte lineage, the EZ-sphere derived astrocytes did not express PAX-6 or βIII tubulin. Flow cytometry indicated that 80 ± 7% of astrocytes and 82 ± 9% of neurons expressed GFAP and βIII tubulin, respectively (Supplementary Figure 1). Astrocytes and neurons differentiated from EZ-spheres for 7, 14, and 21 days were investigated for their capacity to induce barrier properties in iPSC-derived BMECs. Day 14 astrocytes and neurons provided the greatest TEER elevation and were therefore employed for subsequent experiments (Supplementary Figure 2). In addition, astrocytes and neurons continued to express βIII tubulin and GFAP, respectively, following co-culture with iPSC-derived BMECs (Supplementary Figure 1). Taken together, iPSC-sourced EZ-spheres generated populations of BBB-inducing astrocytes or neurons in a relatively short 14-day timeframe.

Co-culture of BMECs with EZ-sphere-derived astrocytes and neurons enhances barrier tightness

Next, iPSC-derived BMECs were co-cultured with EZ-sphere-derived astrocytes and neurons. As described previously, iPSC-derived BMECs express key BBB markers including the endothelial cell marker Pecam, the BBB glucose transporter Glut-1, tight junction proteins, occludin and claudin-5, and the efflux transporter PGP (Lippmann et al. 2012) (Figure 1B). The effects of co-culturing EZ-sphere-derived astrocytes and neurons on barrier formation in purified BMECs were evaluated as outlined in Figure 1C. Importantly, these co-cultures required identification of a common medium suitable for all cell types present. To identify a suitable co-culture medium, iPSC-derived BMECs and co-culture cell types (astrocytes and/or neurons) were differentiated in parallel and placed in co-culture in several media (see Materials and Methods) containing varying amounts of PDS and FBS on day 8 of the BMEC differentiation (Figure 1C). The greatest barrier induction was observed in EC medium containing 1% PDS and 20 ng/mL bFGF (EC +bFGF/+PDS) for the initial 24 h of co-culture (days 8–9), followed by a switch to EC medium containing 1% PDS but lacking bFGF (EC −bFGF/+PDS) for days 9–12, as previously described (Lippmann et al. 2014). To demonstrate that EZ-sphere-derived neurons and astrocytes were capable of inducing BBB properties, they were first co-cultured with primary rat BMECs and barrier formation monitored by TEER (Figure 2A). Monocultured rat BMECs had a TEER value of 86 ± 11 $\Omega \times cm^2$, and when in co-culture with EZ-sphere derived astrocytes the rat BMEC TEER rose to 291 ± 38 $\Omega \times cm^2$ ($p < 0.05$). Similarly, co-culture with EZ-sphere-derived neurons elevated the rat BMEC TEER to 208 ± 21 $\Omega \times cm^2$ ($p < 0.05$). A combination of EZ-sphere-derived neurons and astrocytes (1:3) elevated TEER of rat BMECs to 356 ± 42 $\Omega \times cm^2$ ($p < 0.05$) (Figure 2B). Thus, EZ-sphere-derived neural cells are capable of inducing barrier function in primary rat BMECs.

Since EZ-sphere-derived neural cells induced barrier properties in primary rat BMECs, the effects of EZ-sphere derived astrocytes and neurons on TEER in co-culture models with human iPSC-derived BMECs was systematically examined by comparison with several other inductive and non-inductive cell types (Figures 3A and 3B). Co-culture with EZ-sphere-derived neurons and astrocytes significantly elevated the TEER of iPSC-derived BMECs compared with monoculture (neuron 491 ± 86 $\Omega \times cm^2$ ($p < 0.05$); astrocyte 558 ± 4 $\Omega \times cm^2$ ($p < 0.05$); vs. monoculture 153 ± 9 $\Omega \times cm^2$). Combining EZ-sphere-derived neurons and astrocytes further elevated the TEER compared to co-culture with either astrocytes or neurons alone. A 1:1 ratio of neurons to astrocytes boosted TEER of co-cultured BMECS to 661 ± 41 $\Omega \times cm^2$ ($p < 0.05$) while a 1:3 ratio of neurons to astrocytes further elevated TEER to 886 ± 54 $\Omega \times cm^2$ ($p < 0.05$).

By comparison, primary human neural progenitor cell (NPC)-derived mixtures of astrocytes and neurons (Figure 3A) raised TEER values of co-cultured iPSC-derived BMECs to 611 ± 40 $\Omega \times cm^2$ ($p < 0.05$) (Figure 3B), a similar value as previously reported (Lippmann et al. 2012). Co-culture with primary rat astrocytes also elevated the iPSC-BMEC TEER (784 ± 19 $\Omega \times cm^2$ ($p < 0.05$)) as previously demonstrated (Lippmann et al. 2014). To assess whether the EZ-sphere neural progenitors affected BMEC TEER, we co-cultured undifferentiated EZ spheres with iPSC-derived BMECs. EZ-spheres and EZ-sphere derived

astrospheres that did not yet express astrocyte or neuronal markers (Figure 3A) only modestly elevated TEER compared to monocultured iPSC-derived BMECs (247 ± 33 $\Omega \times cm^2$ (N.S.); 285 ± 12 $\Omega \times cm^2$ ($p < 0.05$), respectively). Finally, mouse 3T3 fibroblasts were used as a non-inductive co-culture control. 3T3 cell co-culture did not elevate TEER with statistical significance (187 ± 14 $\Omega \times cm^2$ (N.S.)) above monocultured BMECs.

We also utilized fluorescein permeability to assess effects of EZ-sphere-derived cells on iPSC-derived BMEC barrier properties (Figure 3C). Monocultured iPSC-derived BMECs exhibited a sodium fluorescein permeability of $P_e=4.8\pm0.3 \times 10^{-7}$ cm/s. Co-culture with EZ-sphere-derived neurons and astrocytes (1:3) resulted in significantly reduced P_e of $1.20\pm0.01 \times 10^{-7}$ cm/s ($p < 0.05$), consistent with the elevated co-culture TEER. Similarly, NPC-derived astrocytes and neurons and primary rat astrocytes significantly reduced fluorescein permeability, indicating a BMEC barrier tightening (NPC-derived neural cells $P_e=2.0\pm1.0 \times 10^{-7}$ cm/s ($p < 0.05$), primary rat astrocytes $P_e=1.9\pm0.1 \times 10^{-7}$ cm/s ($p < 0.05$); respectively). EZ-sphere derived neurons and astrocytes, specifically at a ratio of 1:3, enhanced barrier tightening in BMECs and benchmarked similarly to other non-stem cell-derived human NPCs and rat astrocytes.

Co-culture increases tight junction localization in BMECs

To determine whether the enhanced iPSC-derived barrier properties upon co-culture with EZ-sphere-derived cells were related to structural changes in tight junctions, the localization and continuity of tight junction proteins were examined by immunocytochemistry. iPSC-derived BMECs in monoculture displayed junctions that were frequently discontinuous for occludin and claudin-5 (Figure 4A). Following 48 h of co-culture with EZ-sphere-derived neurons and astrocytes (1:3), the number of cells with discontinuous junctions decreased substantially (Figures 4A and 4B), corresponding to an overall increase in junctional occludin and claudin-5 immunoreactivity (Figure 4C, $83\pm24\%$ increase in occludin and $44\pm14\%$ increase in claudin-5 area fraction indices compared to monoculture ($p<0.05$)). In addition, Western blotting was used to evaluate if co-culture affected tight junction protein expression levels (Figure 4D). Co-culture with EZ-sphere derived neurons and astrocytes resulted in a slight, statistically insignificant increase in occludin and claudin-5 levels compared to monoculture (Figure 4E). Taken together these results indicate that co-culture with EZ-sphere derived astrocytes and neurons enhance barrier properties in iPSC-derived BMECs, and suggest that these changes in barrier properties result from improved formation and maintenance of tight junctions.

BMEC transporters are unchanged by co-culture

The effects of EZ-sphere-derived cell co-culture on PGP efflux transporter activity in iPSC-derived BMECs were investigated by measuring the transport of rhodamine 123 across the iPSC-derived BMEC monolayer. PGP activity was compared between iPSC-derived BMECs in monoculture and iPSC-derived BMECs in co-culture with EZ-sphere-derived neurons and astrocytes (1:3). BMECs in monoculture exhibited increased transport of rhodamine 123 following cyclosporine A (CsA) inhibition ($45\pm8\%$ ($p<0.05$), indicative of the baseline PGP activity in iPSC-derived BMECs (Figure 5A). After co-culture with EZ-sphere derived neurons and astrocytes, PGP activity was statistically indistinguishable from monocultured

iPSC-derived BMECs (40±8% increase in presence of CsA). For comparison, iPSC-derived BMECs in co-culture with primary rat astrocytes, NPC-derived astrocytes and neurons or mouse 3T3 fibroblasts also yielded statistically indistinguishable PGP activities versus iPSC-derived BMEC monocultures. Taken together, these results indicate that PGP is active in the iPSC-derived BMECs as previously described and that co-culture with iPSC-derived or primary-derived astrocytes and neurons does not affect this activity (Lippmann et al. 2012, Lippmann et al. 2014, Wilson et al. 2015). Additionally, co-culture with EZ-sphere derived neurons and astrocytes (1:3) did not affect the localization or expression levels of Glut-1, PGP, MRP-1, BCRP, or the transferrin receptor, TfR (Figures 5B and 5C) (Supplementary Figure 3). Thus, barrier tightening remains the dominant phenotypic effect of co-culturing iPSC-derived BMECs with EZ-sphere derived neurons and astrocytes.

Derivation of an isogenic iPSC-derived human BBB model

Having demonstrated the barrier-enhancing effects of EZ-sphere derived neurons and astrocytes on iPSC-derived BMECs, as indicated by an increase in TEER, reduced permeability, and a decrease in the discontinuous tight junctions, we next investigated the potential of deriving BMECs, astrocytes and neurons from the same donor-derived iPSC line (CS03iCTRn2) to construct an isogenic model of the human NVU. As demonstrated for the IMR90-4 (BMECs) and 4.2-iPSC (astrocytes and neurons) lines above, CS03iCTRn2-derived BMECs, neurons, and astrocytes expressed the appropriate tissue-specific markers (Figures 6A and 6B). Co-culture of CS03iCTRn2-derived BMECs with neurons: astrocytes (1:3) enhanced TEER nearly 4-fold compared to monoculture (785±30 $\Omega \times cm^2$ vs. 201±14 $\Omega \times cm^2$; respectively (p<0.05)), and this barrier was maintained at ~700 $\Omega \times cm^2$ for 5 days (Figure 6C). Barrier tightening was also demonstrated in the isogenic co-culture model as a 13-fold decreased fluorescein permeability compare to monocultured CS03iCTRn2-derived BMECs. (P_e=0.62±0.11 × 10^{-7} cm/s vs. 8.1±0.9 × 10^{-7} cm/s; respectively (p<0.05)) (Figure 6D). PGP-efflux transporter activity in the isogenic model was unaffected by co-culture, with monoculture BMECs displaying a 38±14% increase in rhodamine 1,2,3 transport following CsA inhibition, while co-culture BMECs had a 45±12 % increase in PGP efflux transporter activity (Figure 6E). As with co-cultures derived from mixed iPSC lines (Figures 2–5), we successfully co-cultured BMECs with astrocytes and neurons derived from donor-matched iPSCs and observed enhanced barrier properties in the BMEC population.

Discussion

This study demonstrates that iPSC EZ-sphere-derived astrocytes and neurons can be combined with iPSC-derived BMECs to form a completely human iPSC-derived BBB model comprising these three key NVU cell types. Importantly, many models are chimeric in that they employ cells of the neurovascular unit from differing species. Often, the isolations of each cell type are distinct protocols using tissue from differently aged animals (Lippmann et al. 2013, Deli et al. 2005, Syvänen et al. 2009, Warren et al. 2009). Thus, the technical complexity of multicellular, BBB models can be appreciable. Using iPSC technology, it is possible to derive each human cell type from a single scalable, undifferentiated iPSC source. However, typical protocols for deriving iPSC neurons and astrocytes can take weeks to months to differentiate (Kim *et al.* 2011, Krencik & Zhang 2011), complicating the logistics

of constructing an iPSC-based human BBB model. By contrast, EZ-spheres are a self-renewing pre-rosette neural stem cell population that can be cultured in suspension for prolonged periods of time, passaged via mechanical dissociation techniques, and differentiated to a range of neural lineages in a relatively short time (2 weeks). As demonstrated above, these two-week differentiated neuron and astrocyte populations are capable of substantially improving the barrier properties in iPSC-derived BMECs. Thus, combined with the relatively short BMEC differentiation (8 days), the ability to culture the EZ spheres in self-renewing "intermediate" stage prior to neuron and astrocyte differentiation greatly diminishes the logistical challenges in modeling the BBB with iPSC-derived cells.

The capability of EZ-sphere-derived astrocytes and neurons to enhance BBB properties was first confirmed by their ability to increase in barrier tightness in co-cultured rat BMECs. Subsequently, moving toward co-culture with iPSC-derived BMECs, it was found that EZ-sphere and astrosphere progenitors were not appreciably inductive. However, further differentiated EZ-sphere-derived astrocytes and neurons increased BMEC barrier properties, indicating that neural cell specification is key to BBB induction. Interestingly, we found that co-culture with EZ-sphere-derived astrocytes yielded enhanced barrier induction compared to co-culture with neurons, consistent with previous reports that astrocyte co-cultures were more inductive of BMEC barrier properties than neuronal co-cultures (Schiera *et al.* 2005). BMEC co-culture with a mixture of EZ-sphere-derived astrocytes and neurons yielded even greater improvements in barrier function than either cell type alone, and the most inductive 1:3 ratio of neurons to astrocytes closely resembles the reported distribution in the adult human brain (Azevedo *et al.* 2009, Herculano-Houzel & Lent 2005). In terms of absolute inductive capacity, the EZ-sphere derived astrocytes and neurons compared favorably with other co-culture models. Previously, we demonstrated that TEER is elevated in iPSC-derived BMECs following co-culture with rat astrocytes (700 Ωxcm^2), primary human NPC-derived neurons and astrocytes (450 Ωxcm^2), and primary pericytes followed by NPC-derived neurons and astrocytes (600 Ωxcm^2) (Lippmann et al. 2012, Lippmann et al. 2014). It may be possible to further enhance iPSC-derived BMEC properties by including co-culture with iPSC-derived pericytes, although iPSC-derived pericytes with brain-specific attributes have not yet been reported (Kusuma *et al.* 2015, van der Meer *et al.* 2013). Additionally, manipulation of key BBB signaling pathways could be used to further enhance BBB properties, as we have previously demonstrated with retinoic acid enhancement of iPSC-derived BMEC properties in a pericyte, astrocyte and neuron co-culture model (Lippmann et al. 2014).

The major phenotypic change observed after co-culture was the improved barrier function as observed through TEER and reduced passive permeability. As described previously for hydrocortisone treated rat BMECs, significant changes were not observed in occludin or claudin-5 protein levels, suggesting the presence of sufficient tight junction protein for the observed barrier tightening (Calabria et al. 2006). Alternatively, previous studies have demonstrated a strong correlation between junctional continuity and barrier phenotype (Butt *et al.* 1990, Weidenfeller et al. 2007, Calabria et al. 2006, Weidenfeller *et al.* 2005, Lippmann et al. 2014, Nakagawa et al. 2009). Similar to these studies, upon co-culture with EZ-sphere-derived neurons and astrocytes, there was a significant reduction in the number of

discontinuous junctions in iPSC-derived BMECs. These data indicate that tight junction continuity and not protein expression levels are likely responsible for the observed barrier induction upon co-culture. As another BBB phenotype that could potentially be influenced by co-culture, PGP efflux activity was evaluated. We have previously demonstrated that the iPSC-derived BMECs express functional efflux transporters including PGP, multidrug resistance protein and breast cancer resistance protein (Lippmann et al. 2012, Lippmann et al. 2014, Wilson et al. 2015, Stebbins et al. 2015). Similarly, the iPSC-derived BMECs generated in this study displayed PGP efflux function. Co-culture with EZ-sphere derived astrocytes and neurons had no substantial effect on PGP activity, nor did primary rat astrocyte or primary human NPC-derived astrocyte and neuron co-culture. While a number of studies have demonstrated that co-culture can enhance PGP protein expression and activity levels (Berezowski *et al.* 2004, Dohgu *et al.* 2005, Nakagawa et al. 2009, Perrière *et al.* 2007), other studies reported no changes in PGP expression or activity in immortalized or primary BBB co-culture models, similar to our observations (Freese *et al.* 2014, Lim *et al.* 2007). In addition, given their distinct differentiated origin, it is possible that the iPSC-derived BMECs already possess the appropriate cues for PGP expression unlike primary or immortalized BMEC lines. For instance, while retinoic acid addition can enhance PGP expression and activity in immortalized human and rat brain cell lines (Mizee *et al.* 2013, El Hafny *et al.* 1997), it did not change the PGP activity in iPSC-derived BMECs (Lippmann et al. 2014). Finally, co-culture with EZ-sphere-derived neurons and astrocytes (1:3) did not appear to affect other key BMEC characteristics such as the expression levels of Glut-1, MRP-1, BCRP, or TfR transporters.

Finally, to our knowledge, we have for the first time created an isogenic BBB model where neurons, astrocytes, and BMECs were derived from the same human iPSC line. The isogenic BBB model performed similarly to the models that combined BMECs and EZ-spheres from different sources, and demonstrated elevated TEER and reduced permeability. Additionally, iPSC-derived BMEC co-culture with EZ-sphere-derived astrocytes and neurons resulted in a prolonged elevated TEER compared to previously described models employing primary rat astrocytes and primary human NPCs as co-cultured neural cell sources (Lippmann et al. 2012, Lippmann et al. 2014), thereby increasing the time window for model deployment. It is predicted that the development of such an isogenic BBB model will enable new applications for human BBB models. Specifically, the ability to investigate the impact of genetic human disease on BBB function could prove powerful. Additionally, an iPSC-derived BBB model could be deployed to analyze drug permeability on a patient-by-patient basis thereby contributing to a personalized medicine approach for those suffering with neurological disease.

Supplementary Material

Refer to Web version on PubMed Central for supplementary material.

Acknowledgments

Veterinary Medicine, University of Wisconsin-Madison) for input with EZ-sphere culture and differentiation techniques.

Commonly Used Abbreviations

BBB	Blood Brain Barrier
BMECs	Brain Microvascular Endothelial Cells
NVU	Neurovascular Unit
iPSCs	Induced Pluripotent Stem Cells
TEER	Trans-Endothelial Electrical Resistance
PGP	P-glycoprotein
GFAP	Glial Fibrillary Acidic Protein

References

Azevedo FA, Carvalho LR, Grinberg LT, Farfel JM, Ferretti RE, Leite RE, Jacob Filho W, Lent R, Herculano-Houzel S. Equal numbers of neuronal and nonneuronal cells make the human brain an isometrically scaled-up primate brain. J Comp Neurol. 2009; 513:532–541. [PubMed: 19226510]

Berezowski V, Landry C, Dehouck MP, Cecchelli R, Fenart L. Contribution of glial cells and pericytes to the mRNA profiles of P-glycoprotein and multidrug resistance-associated proteins in an in vitro model of the blood-brain barrier. Brain Res. 2004; 1018:1–9. [PubMed: 15262198]

Brown JA, Pensabene V, Markov DA, et al. Recreating blood-brain barrier physiology and structure on chip: A novel neurovascular microfluidic bioreactor. Biomicrofluidics. 2015; 9:054124. [PubMed: 26576206]

Butt AM, Jones HC, Abbott NJ. Electrical resistance across the blood-brain barrier in anaesthetized rats: a developmental study. J Physiol. 1990; 429:47–62. [PubMed: 2277354]

Calabria AR, Shusta EV. A genomic comparison of in vivo and in vitro brain microvascular endothelial cells. J Cereb Blood Flow Metab. 2008; 28:135–148. [PubMed: 17565361]

Calabria AR, Weidenfeller C, Jones AR, de Vries HE, Shusta EV. Puromycin-purified rat brain microvascular endothelial cell cultures exhibit improved barrier properties in response to glucocorticoid induction. J Neurochem. 2006; 97:922–933. [PubMed: 16573646]

Cecchelli R, Berezowski V, Lundquist S, Culot M, Renftel M, Dehouck MP, Fenart L. Modelling of the blood-brain barrier in drug discovery and development. Nat Rev Drug Discov. 2007; 6:650–661. [PubMed: 17667956]

Deli MA, Ábrahám CS, Kataoka Y, Niwa M. Permeability studies on in vitro blood-brain barrier models: physiology, pathology, and pharmacology. Cell Mol Neurobiol. 2005; 25:59–127. [PubMed: 15962509]

Dohgu S, Takata F, Yamauchi A, et al. Brain pericytes contribute to the induction and up-regulation of blood-brain barrier functions through transforming growth factor-beta production. Brain Res. 2005; 1038:208–215. [PubMed: 15757636]

Ebert AD, Shelley BC, Hurley AM, et al. EZ spheres: a stable and expandable culture system for the generation of pre-rosette multipotent stem cells from human ESCs and iPSCs. Stem Cell Res. 2013; 10:417–427. [PubMed: 23474892]

El Hafny B, Chappey O, Piciotti M, Debray M, Boval B, Roux F. Modulation of P-glycoprotein activity by glial factors and retinoic acid in an immortalized rat brain microvessel endothelial cell line. Neurosci Lett. 1997; 236:107–111. [PubMed: 9404823]

Freese C, Reinhardt S, Hefner G, Unger RE, Kirkpatrick CJ, Endres K. A novel blood-brain barrier co-culture system for drug targeting of Alzheimer's disease: establishment by using acitretin as a model drug. PLoS One. 2014; 9:e91003. [PubMed: 24608847]

Förster C, Burek M, Romero IA, Weksler B, Couraud PO, Drenckhahn D. Differential effects of hydrocortisone and TNFalpha on tight junction proteins in an in vitro model of the human blood-brain barrier. J Physiol. 2008; 586:1937–1949. [PubMed: 18258663]

Herculano-Houzel S, Lent R. Isotropic fractionator: a simple, rapid method for the quantification of total cell and neuron numbers in the brain. J Neurosci. 2005; 25:2518–2521. [PubMed: 15758160]

Janzer RC, Raff MC. Astrocytes induce blood-brain barrier properties in endothelial cells. Nature. 1987; 325:253–257. [PubMed: 3543687]

Kim JE, O'Sullivan ML, Sanchez CA, et al. Investigating synapse formation and function using human pluripotent stem cell-derived neurons. Proc Natl Acad Sci U S A. 2011; 108:3005–3010. [PubMed: 21278334]

Krencik R, Zhang SC. Directed differentiation of functional astroglial subtypes from human pluripotent stem cells. Nat Protoc. 2011; 6:1710–1717. [PubMed: 22011653]

Kusuma S, Facklam A, Gerecht S. Characterizing human pluripotent-stem-cell-derived vascular cells for tissue engineering applications. Stem Cells Dev. 2015; 24:451–458. [PubMed: 25233291]

Lim JC, Wolpaw AJ, Caldwell MA, Hladky SB, Barrand MA. Neural precursor cell influences on blood-brain barrier characteristics in rat brain endothelial cells. Brain Res. 2007; 1159:67–76. [PubMed: 17583679]

Lippmann ES, Al-Ahmad A, Azarin SM, Palecek SP, Shusta EV. A retinoic acid-enhanced, multicellular human blood-brain barrier model derived from stem cell sources. Sci Rep. 2014; 4:4160. [PubMed: 24561821]

Lippmann ES, Al-Ahmad A, Palecek SP, Shusta EV. Modeling the blood-brain barrier using stem cell sources. Fluids Barriers CNS. 2013; 10:2. [PubMed: 23305164]

Lippmann ES, Azarin SM, Kay JE, Nessler RA, Wilson HK, Al-Ahmad A, Palecek SP, Shusta EV. Derivation of blood-brain barrier endothelial cells from human pluripotent stem cells. Nat Biotechnol. 2012; 30:783–791. [PubMed: 22729031]

Lippmann ES, Weidenfeller C, Svendsen CN, Shusta EV. Blood-brain barrier modeling with co-cultured neural progenitor cell-derived astrocytes and neurons. J Neurochem. 2011; 119:507–520. [PubMed: 21854389]

Man S, Ubogu EE, Williams KA, Tucky B, Callahan MK, Ransohoff RM. Human brain microvascular endothelial cells and umbilical vein endothelial cells differentially facilitate leukocyte recruitment and utilize chemokines for T cell migration. Clin Dev Immunol. 2008; 2008:384982. [PubMed: 18320011]

Mizee MR, Wooldrik D, Lakeman KA, et al. Retinoic acid induces blood-brain barrier development. J Neurosci. 2013; 33:1660–1671. [PubMed: 23345238]

Nakagawa S, Deli MA, Kawaguchi H, Shimizudani T, Shimono T, Kittel A, Tanaka K, Niwa M. A new blood-brain barrier model using primary rat brain endothelial cells, pericytes and astrocytes. Neurochem Int. 2009; 54:253–263. [PubMed: 19111869]

Nakagawa S, Deli MA, Nakao S, Honda M, Hayashi K, Nakaoke R, Kataoka Y, Niwa M. Pericytes from brain microvessels strengthen the barrier integrity in primary cultures of rat brain endothelial cells. Cell Mol Neurobiol. 2007; 27:687–694. [PubMed: 17823866]

Perrière N, Yousif S, Cazaubon S, et al. A functional in vitro model of rat blood-brain barrier for molecular analysis of efflux transporters. Brain Res. 2007; 1150:1–13. [PubMed: 17434463]

Sareen D, Gowing G, Sahabian A, et al. Human induced pluripotent stem cells are a novel source of neural progenitor cells (iNPCs) that migrate and integrate in the rodent spinal cord. J Comp Neurol. 2014; 522:2707–2728. [PubMed: 24610630]

Savettieri G, Di Liegro I, Catania C, et al. Neurons and ECM regulate occludin localization in brain endothelial cells. Neuroreport. 2000; 11:1081–1084. [PubMed: 10790886]

Schiera G, Bono E, Raffa MP, Gallo A, Pitarresi GL, Di Liegro I, Savettieri G. Synergistic effects of neurons and astrocytes on the differentiation of brain capillary endothelial cells in culture. J Cell Mol Med. 2003; 7:165–170. [PubMed: 12927055]

Schiera G, Sala S, Gallo A, Raffa MP, Pitarresi GL, Savettieri G, Di Liegro I. Permeability properties of a three-cell type in vitro model of blood-brain barrier. J Cell Mol Med. 2005; 9:373–379. [PubMed: 15963256]

Stebbins MJ, Wilson HK, Canfield SG, Qian T, Palecek SP, Shusta EV. Differentiation and characterization of human pluripotent stem cell-derived brain microvascular endothelial cells. Methods. 2015

Syvänen S, Lindhe O, Palner M, Kornum BR, Rahman O, Långström B, Knudsen GM, Hammarlund-Udenaes M. Species differences in blood-brain barrier transport of three positron emission tomography radioligands with emphasis on P-glycoprotein transport. Drug Metab Dispos. 2009; 37:635–643. [PubMed: 19047468]

van der Meer AD, Orlova VV, ten Dijke P, van den Berg A, Mummery CL. Three-dimensional co-cultures of human endothelial cells and embryonic stem cell-derived pericytes inside a microfluidic device. Lab Chip. 2013; 13:3562–3568. [PubMed: 23702711]

Warren MS, Zerangue N, Woodford K, et al. Comparative gene expression profiles of ABC transporters in brain microvessel endothelial cells and brain in five species including human. Pharmacol Res. 2009; 59:404–413. [PubMed: 19429473]

Weidenfeller C, Schrot S, Zozulya A, Galla HJ. Murine brain capillary endothelial cells exhibit improved barrier properties under the influence of hydrocortisone. Brain Res. 2005; 1053:162–174. [PubMed: 16040011]

Weidenfeller C, Svendsen CN, Shusta EV. Differentiating embryonic neural progenitor cells induce blood-brain barrier properties. J Neurochem. 2007; 101:555–565. [PubMed: 17254017]

Weksler BB, Subileau EA, Perrière N, et al. Blood-brain barrier-specific properties of a human adult brain endothelial cell line. FASEB J. 2005; 19:1872–1874. [PubMed: 16141364]

Wilson HK, Canfield SG, Hjortness MK, Palecek SP, Shusta EV. Exploring the effects of cell seeding density on the differentiation of human pluripotent stem cells to brain microvascular endothelial cells. Fluids Barriers CNS. 2015; 12:13. [PubMed: 25994964]

Yu JY, Vodyanik MA, Smuga-Otto K, et al. Induced pluripotent stem cell lines derived from human somatic cells. Science. 2007; 318:1917–1920. [PubMed: 18029452]

Zhao Z, Nelson AR, Betsholtz C, Zlokovic BV. Establishment and Dysfunction of the Blood-Brain Barrier. Cell. 2015; 163:1064–1078. [PubMed: 26590417]

Zlokovic BV. The blood-brain barrier in health and chronic neurodegenerative disorders. Neuron. 2008; 57:178–201. [PubMed: 18215617]
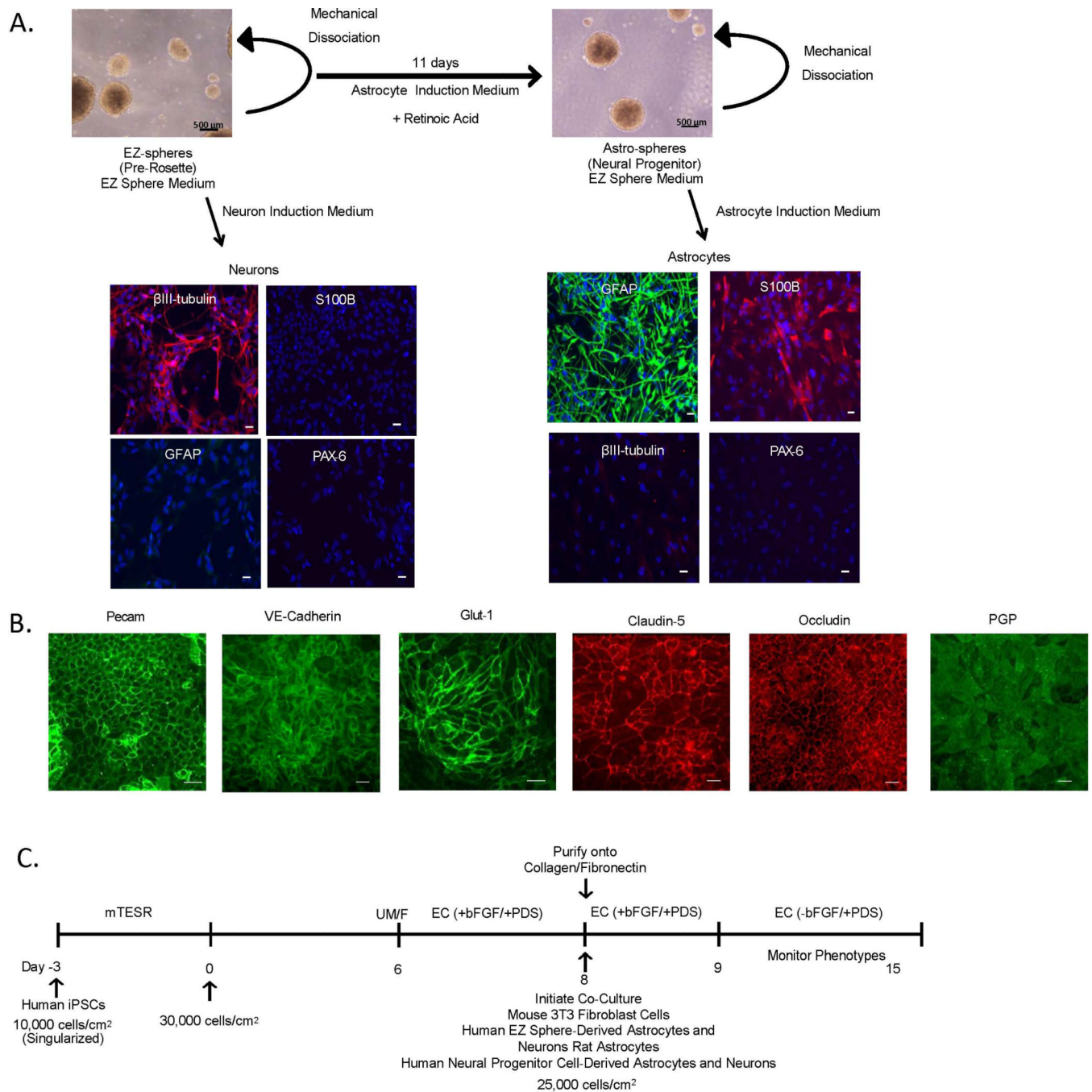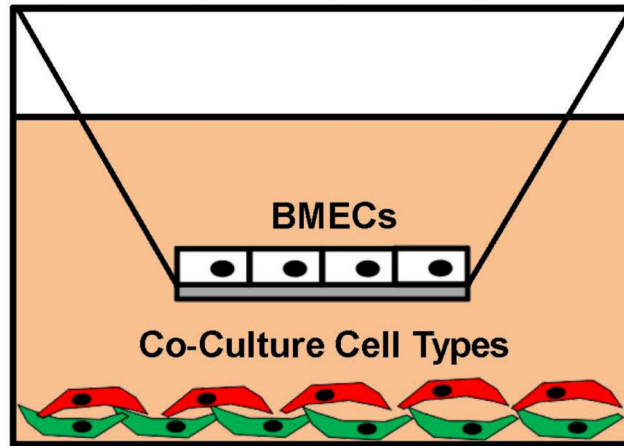
Figure 1. Derivation of neurons, astrocytes and BMECs for BBB modeling
(A) iPSC 4.2 EZ-spheres were maintained in suspension in EZ sphere medium. EZ-spheres were singularized and differentiated towards neurons following a 14-day treatment with neuron induction medium. EZ-spheres were also differentiated further to an astrosphere population following an 11-day treatment with astrocyte induction medium supplemented with retinoic acid. Astrospheres were maintained in suspension in EZ sphere medium and subsequently differentiated to astrocytes following 14 days in an astrocyte induction medium. To examine neuronal and astrocyte differentiation, EZ-sphere-derived cell

populations were immunocytochemically labeled for the early neural ectoderm marker PAX-6, neuronal marker β-III tubulin, and astrocyte markers S100B and GFAP. Scale bar = 200 μm. To derive BMECS, singularized IMR90-4 iPSCs were expanded for 3 days prior to the initiation of differentiation (Day 0), differentiated for six days in UM/F medium and then switched to an EC based medium for two days. (B) IMR90-4 iPSC-derived BMECs were immunolabeled for Pecam and VE-Cadherin, the glucose transporter Glut-1, tight junction proteins Claudin-5 and Occludin, and the efflux transporter PGP. Scale bars = 100 μm. (C) iPSC-BMEC differentiation and co-culture timeline. Day 8 differentiated BMECs were placed in co-culture with EZ-sphere-derived astrocytes or neurons or control cell types including rat astrocytes, human neural progenitor cell-derived astrocytes and neurons, mouse 3T3 fibroblasts. All co-culture experiments were conducted in EC medium with BBB phenotypes being monitored to day 15.
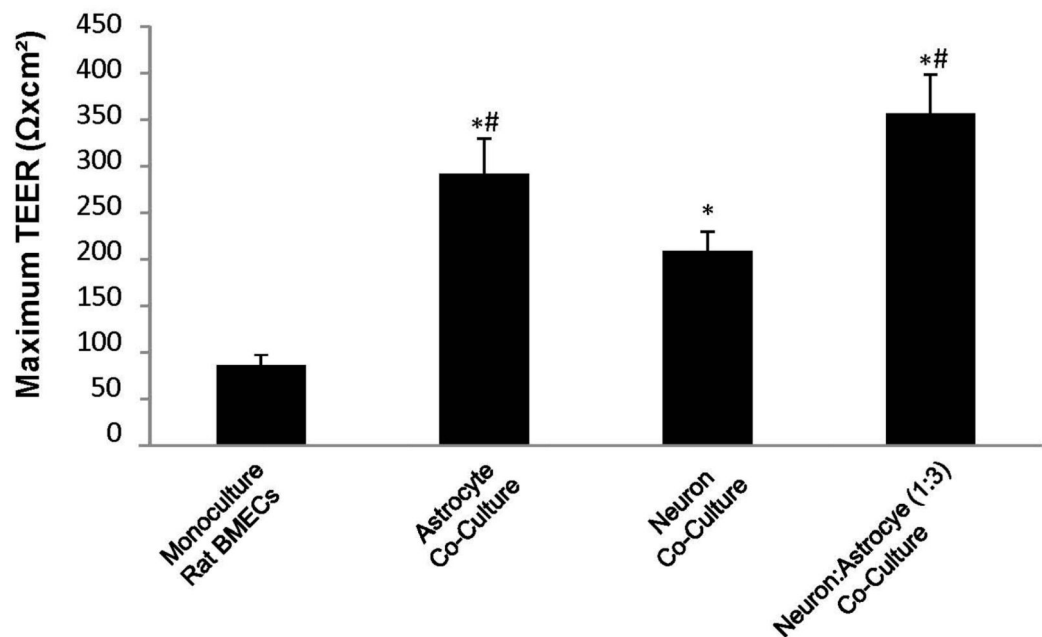
A.

B.

Figure 2. Determination of the BBB inductive effects of EZ-sphere-derived astrocytes and neurons

(A) Co-culture was conducted using a Transwell system. BMECs were seeded on the Transwell filter with co-cultured cell types seeded at the bottom of the well. (B) Primary rat BMECs were co-cultured with iPSC 4.2 EZ-sphere-derived neurons, astrocytes or a mixture of neurons and astrocytes (1 neuron: 3 astrocytes) and TEER was monitored. Statistical significance was calculated using ANOVA.*p<0.05 vs. rat BMECs; #p<0.05 vs. neurons. Values are mean ± SD of three replicates from a single rat BMEC isolation and a single

neuron and astrocyte differentiation, and experiments were repeated for two additional independent isolations and differentiations for verification of reported statistical trends.
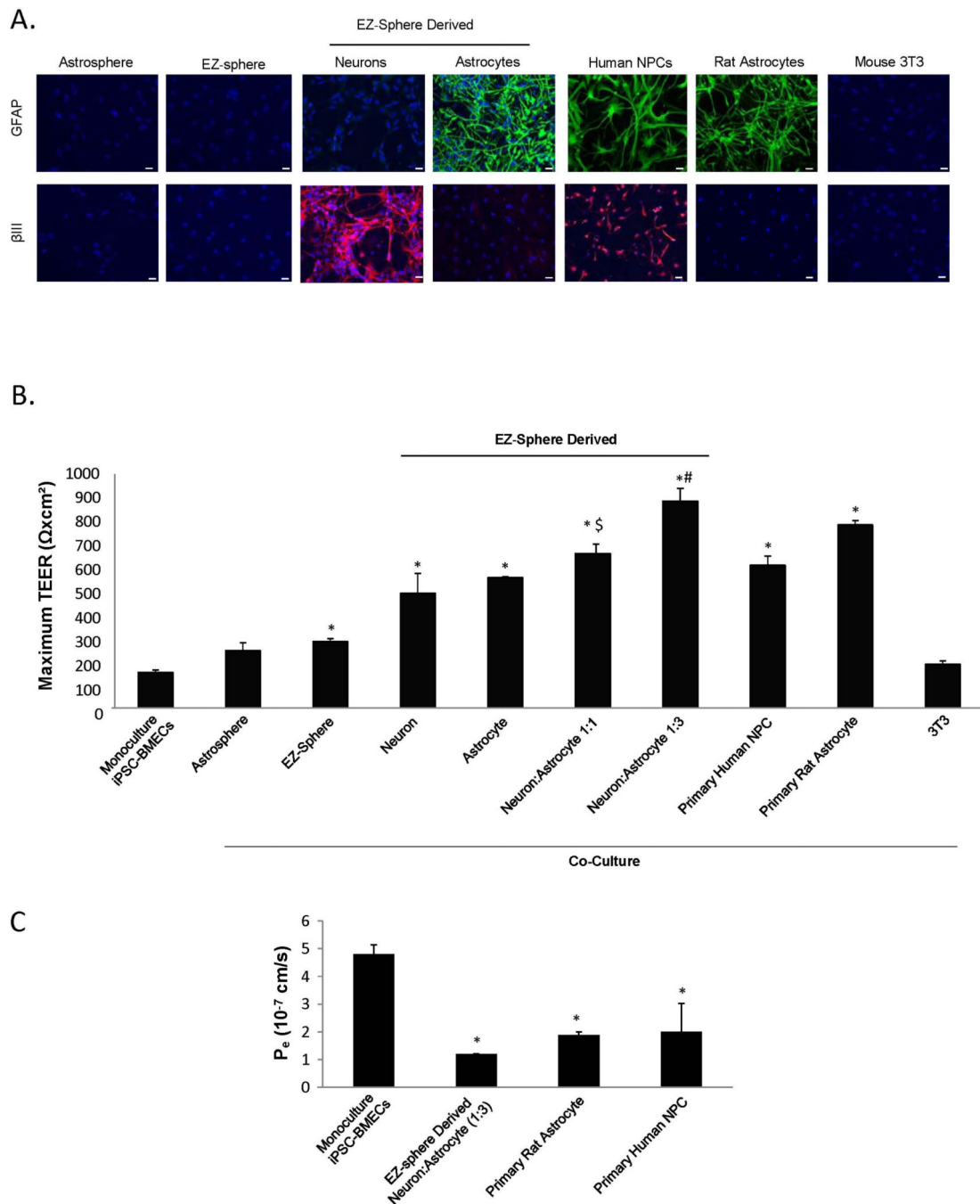
Figure 3. Optimization of co-culture conditions to induce barrier tightening in iPSC-derived BMECs

A variety of co-cultured cells were examined for their capacity to induce barrier tightening in IMR90-4 iPSC-derived BMECs. (A) Immunocytochemical probing for GFAP and β-tubulin III was utilized to examine the distribution of astrocytes and neurons, respectively. Astrospheres, EZ-spheres and EZ-sphere-derived astrocytes and neurons were generated from the iPSC 4.2 EZ-spheres. Primary human NPC-derived mixtures of astrocytes and neurons, primary rat astrocytes and mouse 3T3 fibroblasts were employed as comparative controls. Scale bars = 200 μm. (B) Maximum TEER values were reached 48 h after the

initiation of co-culture (Day 10). All co-cultured cells were seeded at 25,000 cells/cm^2. EZ-sphere-derived neural cells were employed as either pure neuron or astrocyte cultures, or as mixtures as denoted. (C) Fluorescein permeability was measured 48 h following the initiation of co-culture (Day 10). Statistical significance was calculated using ANOVA. *$p<0.05$ vs. monoculture, $^$p<0.05$ vs. neuron or astrocyte co-culture, #$p<0.05$ vs. all groups. Values are mean ± SD of three replicates from a single isolation/differentiation, and experiments were repeated for three additional differentiations for verification of reported statistical trends.
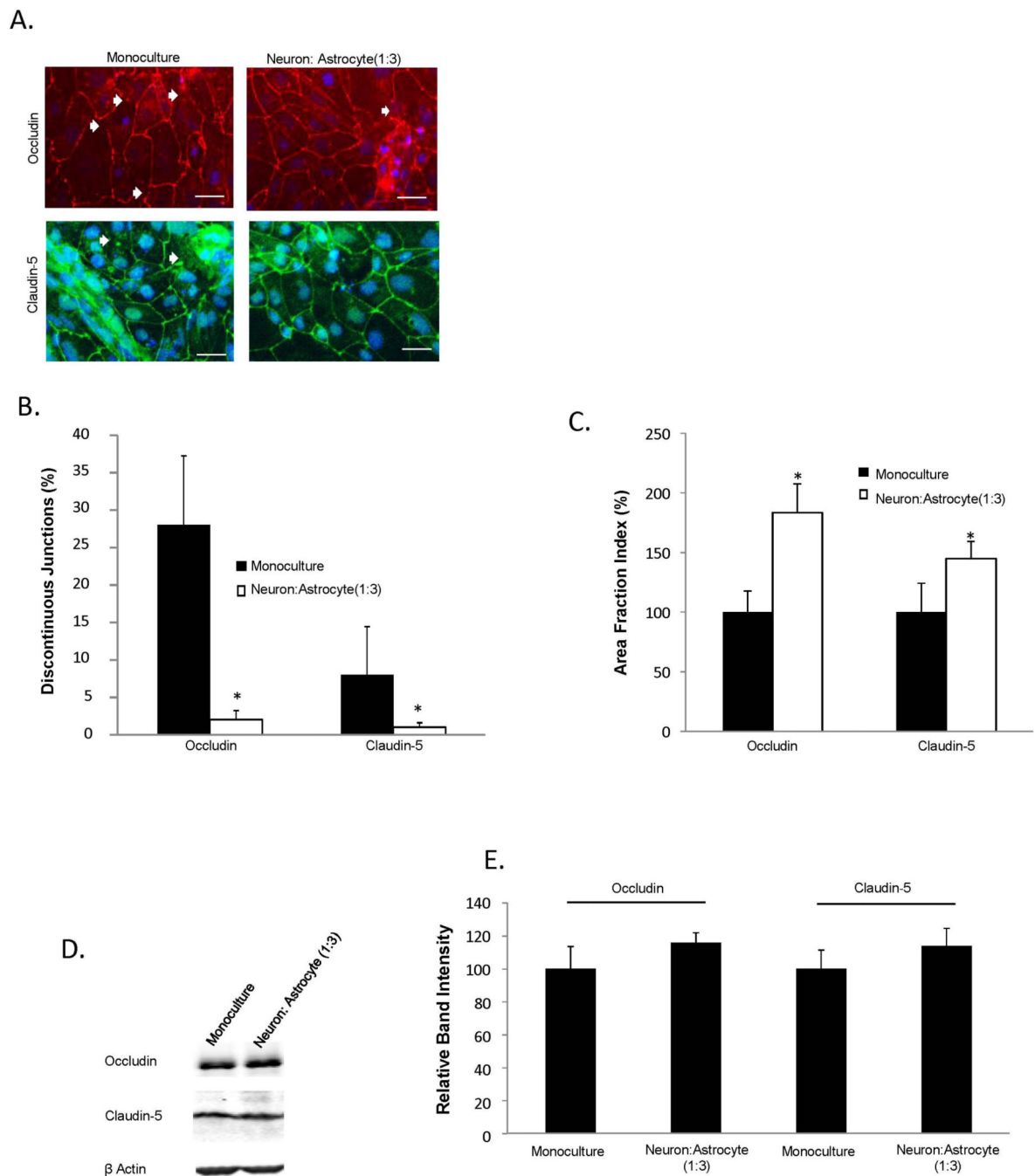
A.

B.

C.

D.

E.

Figure 4. Analysis of tight junction continuity following EZ-sphere co-culture
Tight junction protein localization and expression levels were investigated in IMR90-4 iPSC-derived BMECs following 48 h of co-culture with iPSC 4.2 EZ-sphere-derived neurons and astrocytes (1:3). (A) Immunocytochemistry of occludin and claudin-5 revealed discontinuous tight junctions (white arrows). Scale bars = 50 μm. (B) Discontinuous junctions were quantified in BMECs in monoculture and co-culture conditions by counting cells that contained at least one discontinuous tight junction. (C) Additional quantification of tight junction localization in BMECs in monoculture and co-culture conditions was

conducted by calculating the area of each image having occludin and claudin-5 immunoreactivity, resulting in the area fraction index. The data is normalized to monoculture conditions and expressed as a percentage. Statistical significance for panels (B) and (C) was calculated using a Student's t-test. *p<0.05 vs. monoculture. Values are mean ± SD of three blinded independent differentiations. (D) Western blot of tight junction proteins occludin and claudin-5 in both monoculture and co-culture conditions with a β-actin loading control. A single lane representative of triplicate Western blot samples is shown. (E) Quantification of Western blots to compare tight junction protein expression levels. Co-culture samples were independently normalized to each respective monoculture sample. Statistical significance was calculated using a Student's t-test. Values are mean ± SD of three independent differentiations.
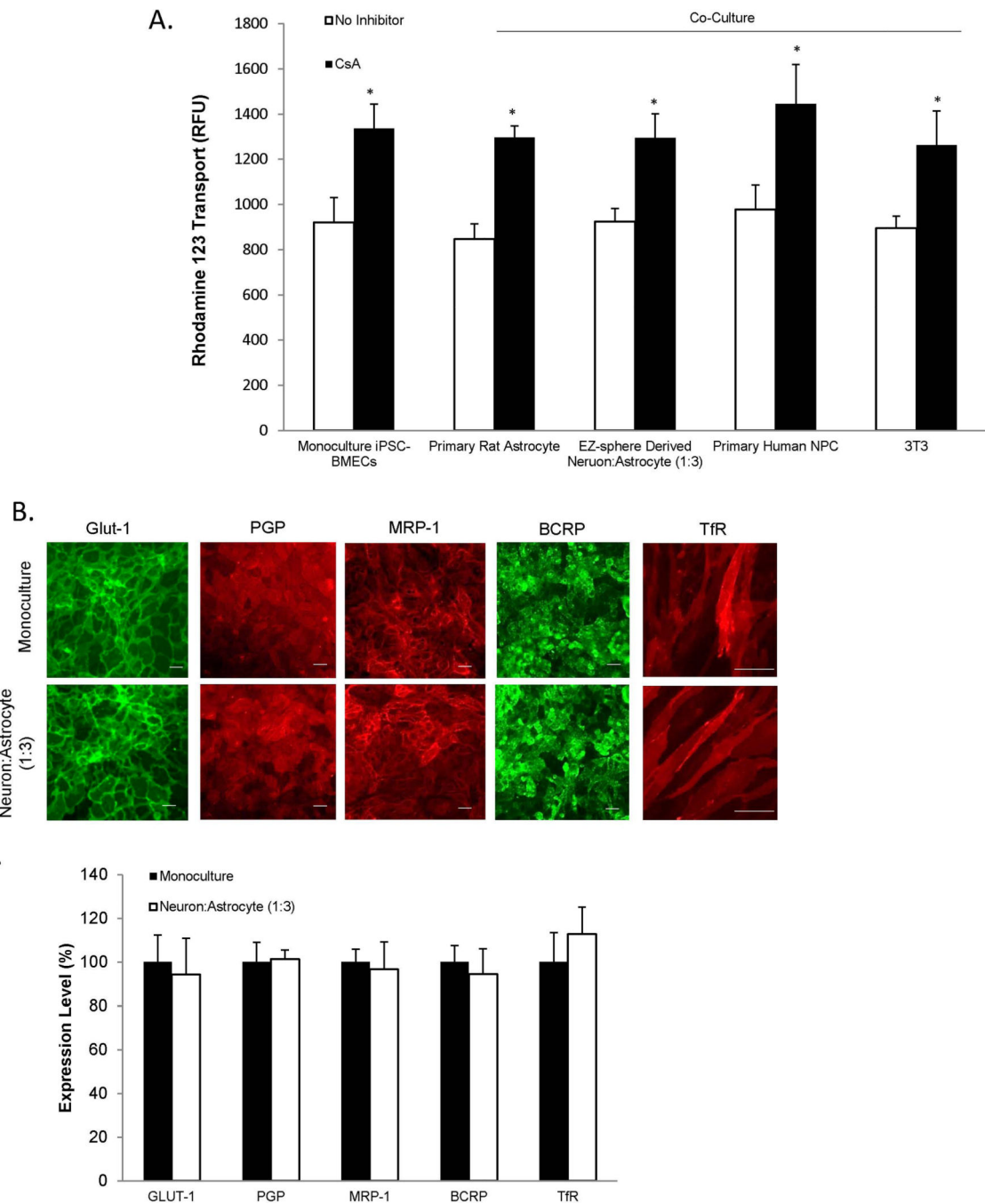
Figure 5. Evaluation of BMECs following co-culture

(A) To assess active efflux transporter activity in IMR90-4 iPSC-derived BMECs, the trans-BMEC transport of PGP substrate rhodamine 123, with and without the PGP inhibitor cyclosporine A (CsA) was measured. IMR90-4 iPSC-derived BMECs were co-cultured with rat astrocytes, human NPC-derived astrocytes and neurons, iPSC 4.2 EZ-sphere-derived neurons and astrocytes (1:3), or mouse 3T3 fibroblasts. Rhodamine 123 transport from the apical to the basolateral chamber was measured in the two-compartment co-culture model in the presence or absence of CsA and reported as raw fluorescence units (RFU). Statistical

significance was calculated using ANOVA.*p<0.05 vs. no inhibition control for each experimental condition. Values are mean ± SD of three replicates from a single differentiation/isolation, and experiments were repeated for two more additional independent differentiations to confirm statistical trends. (B) Immunocytochemistry of IMR90-4 iPSC-derived BMECs in mono-culture or after 48 hours of co-culture with 4.2 iPSC EZ-sphere-derived neurons and astrocytes (1:3) probing for glucose transporter, Glut-1, efflux transporters, PGP, MRP-1, BCRP, or transferrin receptor, TfR, expression. Scale bar = 100 µm. (C) Quantitative transporter expression levels were determined using flow cytometry. Geometric means of positively immunolabeled cell populations were used to compare expression levels with and without co-culture. Sample flow cytometry data can be found in Supplementary Figure 3. The data are normalized to monoculture expression levels. Statistical significance was determined using a Student's t-test. Values are mean ± SD of three independent differentiations.
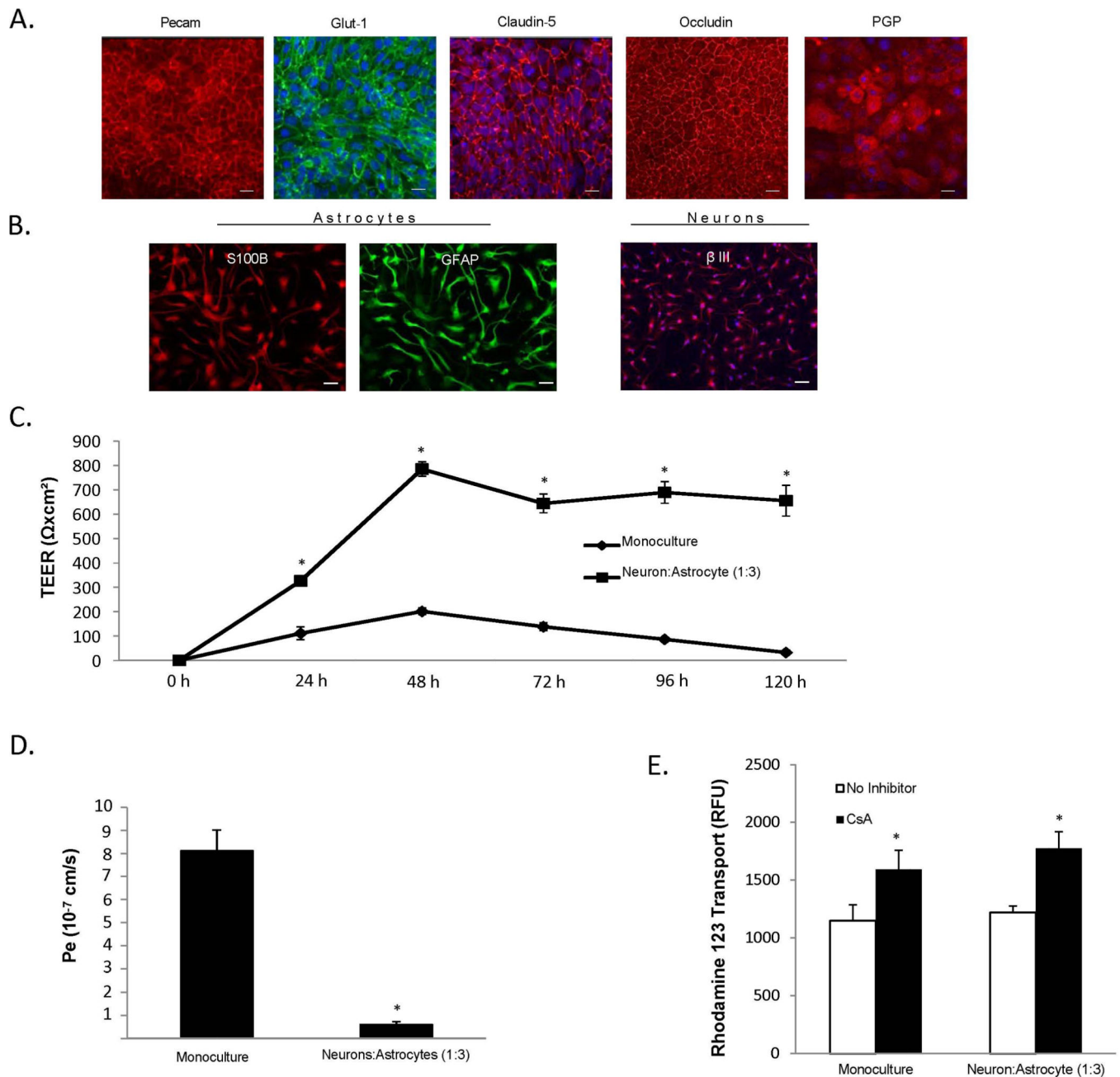
Figure 6. Development of an isogenic neurovascular unit
iPSC-derived BMECs and EZ-sphere-derived astrocytes and neurons were differentiated from the same CSO3n2 iPSC line. (A) Immunocytochemical analysis of BBB markers in CSO3n2-derived BMECs. Scale bar = 100 μm. (B) Immunocytochemical of astrocyte and neuron markers in astrocytes and neurons differentiated from CSO3n2 EZ-spheres. Scale bars = 100μm. (C) Temporal TEER profile for CSO3n2 iPSC-derived BMECs with and without co-culture with CS03n2 iPSC-derived neurons and astrocytes. Statistical significance was calculated using Student's t-test. *p<0.05 vs. monoculture. Values are mean ± SD of three replicates from a single differentiation, and experiments were repeated for two additional independent differentiations to verify statistical trends. (D) Sodium fluorescein

permeability measured at 48 h after the initiation of co-culture. Statistical significance was calculated using Student's t-test. *p<0.05 vs. monoculture. Values are mean ± SD of three replicates from a single differentiation, and experiments were repeated for two additional independent differentiations to verify statistical trends. (E) PGP efflux transporter activity was measured 48 h after initiation of co-culture. Statistical significance was calculated using ANOVA. *p<0.05 vs. no-inhibition. Values are mean ± SD of three replicates from a single differentiation, and experiments were repeated for two additional independent differentiations to verify statistical trends.